Effect of nitrogen and vacancy defects on the thermal conductivity of diamond: An *ab initio* Green's function approach

N. A. Katcho*
CIC EnergiGUNE, Albert Einstein 48, 01510 Miñano, Álava, Spain

J. Carrete
LITEN, CEA-Grenoble, 17 rue des Martyrs, 38054 Grenoble Cedex 9, France

Wu Li
Scientific Computing & Modelling NV, De Boeleaan 1083, 1081 HV Amsterdam, Netherlands

N. Mingo
LITEN, CEA-Grenoble, 17 rue des Martyrs, 38054 Grenoble Cedex 9, France

(Received 10 June 2014; revised manuscript received 3 September 2014; published 29 September 2014)

We show that impurities and vacancies affect the thermal conductivity much more strongly than what is predicted by widely accepted models. When local distortions around point defects are strong, standard perturbative approaches fail, and phonon scattering can only be accounted for by an exact Green's function calculation. We apply the theory to the study, from first-principles, of nitrogen and vacancy defects in diamond. The thermal conductivity is computed by solving the linearized Boltzmann transport equation. The Born approximation underestimates the phonon scattering cross sections of nitrogen and vacancies by factors of 3 and 10, respectively. Thermal conductivity calculations are in good agreement with experiment.

DOI: 10.1103/PhysRevB.90.094117 PACS number(s): 63.20.kp, 61.72.−y, 63.20.dk

I. INTRODUCTION

Thermal conductivity κ is currently the focus of intense research [1,2] due to its crucial role in many technologies. For example, microelectronic cooling requires materials with high κ [1], whereas very low κ is desired for high-efficiency thermoelectric materials [3]. From a structural point of view, these materials can be quite complex [4]. Alloying, matrix precipitates, grain boundaries, and finite size are some of the structural features present in these materials that strongly influence κ. An accurate computation of κ is then essential to quantify the effect of the different scattering sources, to understand experimental results, and to investigate new materials with targeted applications.

For insulators and many semiconductors, it is usually enough to compute the lattice thermal conductivity κ_L since in these systems most of the heat is carried by phonons. κ_L can be computed by solving the Boltzmann transport equation (BTE), an approach that has proven to be very fruitful in understanding thermal transport [5]. Before the advent of modern computers, exact solutions of the BTE were unfeasible, and crude approximations for both phonon dispersion and scattering rates were needed [6,7]. Although these approximations afford poor predictive power, they make quantitative estimates possible and are useful in the interpretation of experimental results [8–10]. Parametrized and *ab initio* numerical solutions of the BTE have been obtained in recent years for bulk crystals [11–14], proving that the BTE can provide very accurate estimates of κ_L. SHENGBTE, a software package based on a full iterative solution of the BTE for any crystalline bulk material, was released recently [15–17]. Despite all this progress in the *ab initio* computation of κ_L there are still problems that must be addressed, such as the calculation of the phonon scattering arising from the presence of structural defects. For a long time, the theoretical treatment has been based on the work of Klemens [18], who obtained analytical expressions for the elastic scattering cross section σ of point defects, dislocations, and grain boundaries using perturbation theory. To keep the problem tractable analytically, such calculations were restricted to the long-wavelength limit, and simplified assumptions about crystal structure and atomic interactions were made. An extension to the whole frequency range, by interpolating between σ for the long- and short-wavelength limits, has been suggested [19]. Recently, an exact calculation of σ using the Green's function approach has been proposed [20–22]. The main limitation is the requirement of a localized perturbation in real space and a low concentration of defects to make multiple scattering between them negligible. Otherwise, some approximations are needed, for example, the virtual crystal approximation in the case of nondilute alloys [7]. Also molecular dynamics simulations with interatomic force constants (IFCs) obtained from first principles represent an alternative [23].

Among structural defects, point defects are best suited for the Green's function approach. The perturbation they induce is localized in a small region around the defect, and usually their concentration is very low, on the order of thousands of parts per million. An important case is the vacancy, for which an accurate computation of σ has not yet been carried out. Previous theoretical calculations were based on low-order perturbation theory and simplified phonon bands [24,25]. In addition, these studies did not compute the change in IFCs and its effect on the phonon scattering. They only considered a mass perturbation, which greatly simplifies the problem. However, for vacancies the changes in IFCs are large and cannot be neglected. For this reason, it was proposed to set

*nayape@cicenergigune.com

the perturbing mass to three times the host mass [25] rather than equal to the host mass [24]. A recent work [26] was still based on the seminal work of Klemens with only a mass perturbation term, although the calculation was refined by estimating bond relaxation effects. Here we demonstrate how such traditional perturbative approaches fail for vacancies and for any perturbation for which changes in harmonic IFCs are large. In addition, we avoid the use of any effective mass by computing directly the changes in IFCs from first principles. To test the theory, we have studied diamond because available experimental data relate κ_L to the N and vacancy concentrations. Both kinds of defects strongly affect the κ_L of diamond, mainly due to harmonic IFCs effects.

II. METHODS

In the harmonic approximation, the dynamical equation for the vibrational modes can be expressed as

$$\omega^2 u_{i\alpha} = \sum_{j\beta} \frac{K_{i\alpha,j\beta}}{(M_i M_j)^{1/2}} u_{j\beta}, \tag{1}$$

where ω is the mode frequency, $u_{i\alpha}$ is the mass-normalized atomic displacement of atom i in direction α, and K and M refer to the corresponding harmonic IFCs and atomic masses. When a substitutional impurity is introduced, generally, the mass and IFCs involving the impurity are different from those of the host lattice. In the general case two terms must be added to the right-hand side of Eq. (1): a mass term, $V_M = -\frac{M_i' - M_i}{M_i}\omega^2$, and an IFC term, $V_K = \frac{K'_{i\alpha,j\beta} - K_{i\alpha,j\beta}}{(M_i M_j)^{1/2}}$, where the prime refers to the values of the system with the impurity. V_K must obey the translational invariance rule [27], and when it is computed numerically or approximated using some cutoff radius to limit the size of the matrix, this symmetry must be enforced. This can be done by adding small corrections to the harmonic IFCs of the perturbed system. These corrections can be computed by applying the Lagrange multiplier method as proposed in Ref. [5].

The procedure to calculate σ using the Green's function approach is explained in detail in Ref. [21]. Here we summarize the main formulas. σ is expressed as

$$\sigma = \frac{\Omega}{\omega v} \sum_{q'} |\langle q'|T^+(\omega^2)|q\rangle|^2 \delta(\omega'^2 - \omega^2), \tag{2}$$

where $|q\rangle$ and $|q'\rangle$ represent the incident and scattered phonons, respectively. Ω is the volume into which $|q\rangle$ is normalized, and v is the group velocity of $|q\rangle$. T^+ is the T matrix, defined by

$$T^+ = (I - VG_0^+)^{-1} V, \tag{3}$$

where I is the identity matrix, V is the perturbation matrix, and G_0^+ is the retarded Green's function of the unperturbed system. In the general case, $V = V_M + V_K$. An important point concerns the frequency dependence of the perturbation matrix. V_M scales as ω^2, and it becomes smaller and smaller as the frequency approaches zero. A low-order perturbative approach, such as the Born approximation, is then justified at low frequency. However, the situation for V_K is different since this term does not depend on frequency. If changes in IFCs are large, the perturbation cannot be considered small at any frequency.

Once σ is calculated, we use SHENGBTE to compute the phonon lifetimes τ_λ and κ_L by solving the linearized BTE. Technical details are given in Ref. [15].

III. RESULTS

A. Failure of the low-order perturbative approach

As a reference model for the following discussion, we consider the one-dimensional (1D) monoatomic chain. In its simplest form, all the atoms of the chain are of the same type, with mass M, and only first-neighbor interactions are included, with a harmonic IFC denoted by K. We consider the following perturbation. Given an atom at site i, we modify its bonds with atoms at sites $i-1$ and $i+1$ by decreasing K to K'. The perturbation matrix is a 3×3 matrix whose elements are

$$V = \begin{bmatrix} \frac{\Delta K}{M} & -\frac{\Delta K}{M} & 0 \\ -\frac{\Delta K}{M} & \frac{2\Delta K}{M} & -\frac{\Delta K}{M} \\ 0 & -\frac{\Delta K}{M} & \frac{\Delta K}{M} \end{bmatrix}, \tag{4}$$

where $\Delta K = K' - K$. A vacancy is created when $\Delta K = -K$. The Green's function G_0^+ can also be calculated analytically [28]. Once V and G_0^+ have been computed, the T matrix and σ are obtained using Eqs. (3) and (2), respectively. In one dimension the incident phonon can be either transmitted or reflected. Then σ can also be expressed in terms of the reflection (ρ) and transmission (τ) coefficients as [28] $\sigma = |\tau - 1|^2 + |\rho|^2$. When $\Delta K = -K$, the atom at site i is completely disconnected from its neighbors, and then the phonon cannot be transmitted. Note that this conclusion does not depend on the actual mass of the impurity. For $\Delta K = -K$ and no matter what ΔM is, we have $\tau = 0$, $\rho = 1$, and $\sigma = 2$ for all phonons. Therefore for the vacancy case V_K is the only term affecting the scattering since ΔM can always be set to zero. There is no mention of this fact in the previous perturbative studies, where V_M is invariably set to ω^2 and seems to play a role in the scattering. Figure 1(a) shows σ as a function of ω for different values of ΔK, calculated

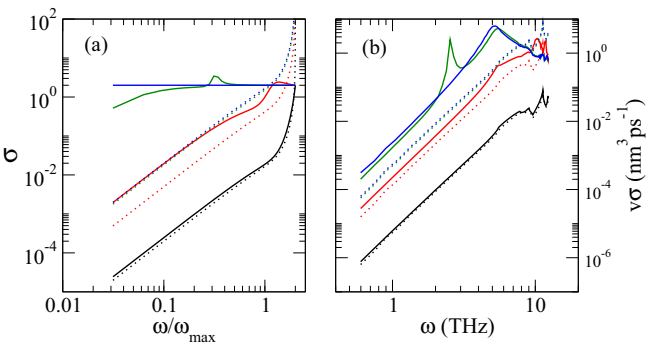

FIG. 1. (Color online) (a) Cross section for the 1D chain. (b) Cross section times group velocity for Si Keating potential, longitudinal phonon branch along the [100] direction. Solid line: T-matrix calculation. Dotted line: Born approximation. From bottom to top: $\Delta K/K = -0.10$ (black), -0.50 (red), -0.95 (green), -1.00 (blue).

using both the T matrix and the Born approximation. As ΔK approaches -1, the failure of the Born approximation becomes more dramatic. It can be seen that in this case the T-matrix calculation shows a strong peak in σ at low ω, which is absent from the perturbative calculation. This is the signature of a low resonance state, and it explains why the perturbative approach fails since it cannot be applied when resonances appear.

A much more realistic but still simple model is the Keating potential [29], which was developed to describe the elastic energy in diamond and zinc-blende crystal structures. In this model a vacancy is created by removing the interaction of one atom with its 4 nearest and 12 second-nearest neighbors. Neglecting the relaxation after the creation of the vacancy, the perturbation matrix can still be obtained analytically, but the Green's function must be obtained by numerical integration. In this work we have used the tetrahedron approach of Lambin and Vigneron [30]. Figure 1(b) shows v times σ as a function of ω for Si at the same $\Delta K/K$ ratios as for the 1D chain. A picture with similarities to the 1D case is obtained. Again, just before the creation of a vacancy ($\Delta K/K = 0.95$), the large differences in IFCs between the host and the impurity give rise to a resonance state that shows up in the cross section as a strong peak. However, the effect is less dramatic than in one dimension since in three dimensions the creation of a vacancy cannot totally disconnect one part of the crystal from the other. Thus it is clear that when dealing with vacancies or, more generally, large variations in IFCs, a perturbative approach cannot provide an accurate description of σ, and a T-matrix approach must be used.

B. *Ab initio* modeling of N and vacancy defects in diamond

We have modeled point defects using the supercell approach. All density functional theory (DFT) calculations in this work were carried out in the generalized gradient approximation (GGA), using the projector-augmented-wave pseudopotentials supplied by VASP [31]. The energy cutoff was set to 500 eV, and we used a $4 \times 4 \times 4$ supercell and a $2 \times 2 \times 2$ **k**-point grid for both the impurity and the bulk systems. The supercell volume was set to the diamond bulk value predicted by VASP.

Nitrogen is the main impurity in natural and many synthetic diamonds. They are classified as type I or II depending on whether they contain substantial amounts of N or not. If N is mainly aggregated, as dimers (A center) or associated with vacancies (N3 and B centers), it is classified as type Ia. On the other hand, if N is arranged as neutral single substitutional impurities (C center), the diamond is classified as type Ib. Type Ib is paramagnetic and shows electron spin resonance, while type Ia does not. In our calculations we have considered N to be an isolated substitutional impurity, i.e., type Ib.

The C center has been extensively studied by magnetic resonance techniques [32]. It is well established that the point symmetry around the N changes from T_d to C_{3v}. The distortion which lowers the symmetry consists of an elongation of one N-C bond along one of the $\langle 111 \rangle$ directions, which becomes the C_{3v} principal symmetry axis. As the N and C atoms move away from each other towards the plane of their other three neighbors, these three bonds are shortened. To obtain the correct point symmetry around the impurity, after

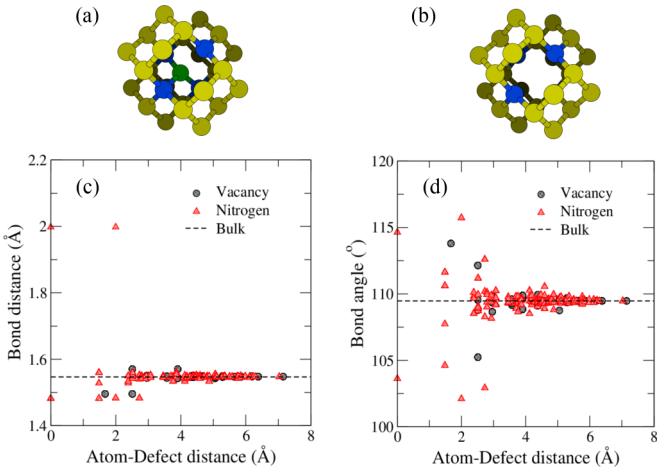

FIG. 2. (Color online) (a) and (b) The [100] projection view of the N impurity and vacancy defects after the *ab initio* relaxation. Green: N atom. Blue: first coordination shell. Yellow: second and third coordination shells. (c) and (d) Bond distances and angles as a function of the distance to the defect. Dashed line: bulk values for diamond, 1.547 Å and 109.47°.

substitution of one C atom by N, the N atom was slightly displaced from its site along one $\langle 111 \rangle$ direction. Then we carried out a relaxation of all the atoms of the supercell. The results of the *ab initio* relaxation are shown in Fig. 2. It can be seen that the perturbation extends up to around 5 Å away from the impurity. The short N-C bond distance is 1.482 Å, and the long one is 1.998 Å, 29% longer than the bond distance in bulk diamond. The bond angle for N is 114.6°, whereas for the tricoordinated C it is 115.7°. These structural parameters are in agreement with previous first-principles calculations [33,34].

For the neutral vacancy a Jahn-Teller distortion which reduces the point symmetry from T_d to D_{2d} is expected [35]. This distortion can be accomplished by moving pairs of first neighbors closer together along the corresponding $\langle 110 \rangle$ direction. However, when in our calculations the system is relaxed after the D_{2d} symmetry is imposed, the T_d symmetry is recovered. This is in agreement with previous *ab initio* calculations [36], where it was reported that the D_{2d} symmetry is obtained in Si but not in C. They found that the four nearest neighbors move outwards 0.12 Å along the corresponding $\langle 111 \rangle$ direction, in perfect agreement with our results. For the tricoordinated C atoms, the bond distance is reduced from 1.547 to 1.496 Å, and the bond angle increased from 109.7° to 113.8°, as it must be expected from a reduction in the coordination number.

C. Thermal conductivity of diamond with N and vacancy defects

Harmonic and anharmonic IFCs were computed using the small-displacement method. We used a $4 \times 4 \times 4$ supercell. From the DFT results, harmonic and anharmonic IFCs were obtained using PHONOPY [37] and THIRDORDER.PY [15], respectively. Interactions up to fourth-nearest neighbors were considered for the anharmonic IFCs. The perturbation matrix was built from the difference between the two sets of harmonic

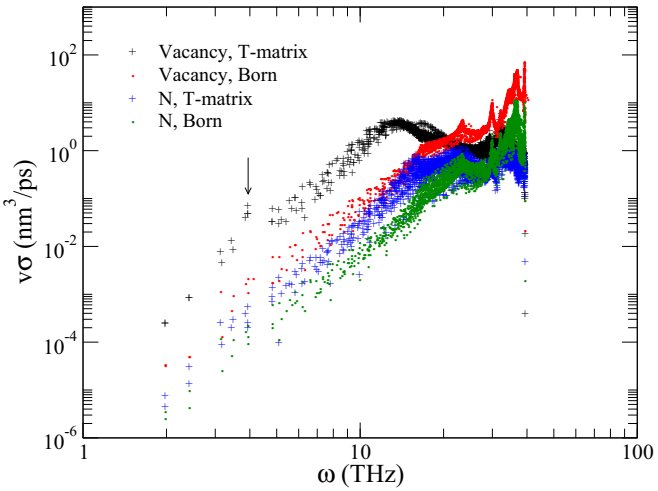

FIG. 3. (Color online) Cross sections times group velocity for substitutional N and vacancy defects in diamond, derived from the T matrix and from the Born approximation. The arrow points at the resonance state (see text for details).

IFCs (defect and bulk). We have considered changes in harmonic IFCs for first- and second-nearest-neighbor interactions of all atoms belonging to the six nearest shells around the defect (∼4.5 Å cluster radius around the defect). The cross section times group velocity is shown in Fig. 3. It can be seen that the Born approximation fails at low frequency by factors of around 3 and 10 for N and the vacancy, respectively. This is because V_K is frequency independent and changes in harmonic IFCs are large. For the vacancy case there is a small resonance peak at 4 THz (arrow in Fig. 3) since the vacancy was not totally disconnected from the lattice. An extrapolation at low frequency can be used to overcome this problem. Comparing our results with the previous work of Ratsifaritana and Klemens [25], we find that the T-matrix result is reproduced at low frequency using $\Delta M = -6M$, twice the value suggested by them.

To compute κ_L we used a $28 \times 28 \times 28$ **q** grid to reach convergence. Figure 4 shows κ_L of diamond as a function

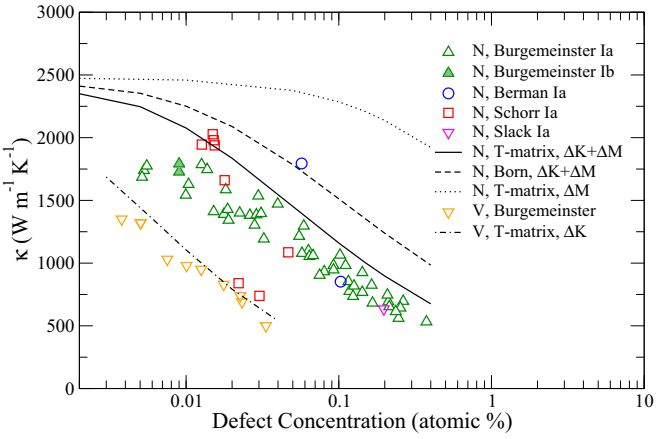

FIG. 4. (Color online) κ_L of diamond as a function of defect concentration. N and V stand for nitrogen and vacancy, respectively.

of N content. The theoretical curves demonstrate that the decrease in κ_L is mainly due to changes in the harmonic IFCs. The same calculation was done by Turk and Klemens [38]. They suggested a factor of around 3.5 between V_K and V_M contributions, whereas we found a somewhat larger difference, a factor of 5. For N content higher than 0.1% the differences between taking into account changes in harmonic IFCs and not taking them into account can be as large as 200%–300%. On the other hand, the Born approximation overestimates κ_L by 40% for the highest N content. When compared with experimental data [39–42], the T-matrix calculation overestimates κ_L by just 25%. Most of the experimental data correspond to type Ia. The few type Ib data we have found seem to indicate that no significant differences exist between types Ia and Ib. However, the existence of other types of defects in experimental samples has been reported [40]. Spikes on x-ray diffraction patterns were ascribed to planar defects in {100} planes, and platelets were shown by transmission electron microscopy. Nickel atoms were detected on type Ib diamonds. The existence of defects other than single substitutional N could explain the small discrepancies between theory and experiment.

For the vacancy case, we have only found one experimental work where measurements of κ_L as a function of single-vacancy concentration has been reported [43]. Figure 4 shows that the agreement with our calculations is rather good. The theoretical curve corresponding to the Born approximation is not plotted for the sake of clarity. For the highest concentration, 0.04%, the Born approximation overestimates the T-matrix result almost by a factor of 2.

IV. CONCLUSIONS

The standard theoretical approaches used to study phonon scattering by defects, based on low-order perturbation theory, fail when they are applied to perturbations where changes in IFCs are large, underestimating the cross sections. In these cases the perturbation matrix is mainly described by V_K, which does not depend on ω. This explains why V_K does not become small at low frequency and why perturbative approaches fail. Large changes in IFCs must be expected when bonds are broken (vacancies), formed (interstitials), or strongly distorted (atomic substitution by atoms with different bonding properties, such as atoms belonging to different groups of the periodic table). In these systems the T-matrix approach is required. In the particular case of vacancies, we have shown that V_M has no influence as long as the atom at the vacancy site is totally disconnected from the lattice. Therefore, to compute the phonon scattering arising from vacancies only V_K must be taken into account. Our results show good agreement with experiment, which singles out this method by virtue of its predictive power.

ACKNOWLEDGMENTS

We are grateful to D. A. Broido and L. Lindsay for fruitful discussions. This work was supported by the EU FP7 (NEAT, Grant No. 263440) program.

[1] D. G. Cahill, W. K. Ford, K. E. Goodson, G. D. Mahan, A. Majumdar, H. J. Maris, R. Merlin, and S. R. Phillpot, J. Appl. Phys. **93**, 793 (2003).

[2] D. G. Cahill, P. V. Braun, G. Chen, D. R. Clarke, S. Fan, K. E. Goodson, P. Keblinski, W. P. King, G. D. Mahan, A. Majumdar, H. J. Maris, S. R. Phillpot, E. Pop, and L. Shi, Appl. Phys. Rev. **1**, 011305 (2014).

[3] M. Zebarjadi, K. Esfarjani, M. S. Dresselhaus, Z. Ren, and G. Chen, Energy Environ. Sci. **5**, 5147 (2012).

[4] K. Biswas, J. He, I. D. Blum, C.-I. Wu, T. P. Hogan, D. N. Seidman, V. P. Dravid, and M. G. Kanatzidis, Nature (London) **489**, 414 (2012).

[5] N. Mingo, D. A. Stewart, D. A. Broido, L. Lindsay, and W. Li, in *Length-Scale Dependent Phonon Interactions* (Springer, Berlin, 2014), pp. 137–173.

[6] J. Callaway, Phys. Rev. **113**, 1046 (1959).

[7] B. Abeles, Phys. Rev. **131**, 1906 (1963).

[8] M. Asen-Palmer, K. Bartkowski, E. Gmelin, M. Cardona, A. P. Zhernov, A. V. Inyushkin, A. Taldenkov, V. I. Ozhogin, K. M. Itoh, and E. E. Haller, Phys. Rev. B **56**, 9431 (1997).

[9] W. Kim, J. Zide, A. Gossard, D. Klenov, S. Stemmer, A. Shakouri, and A. Majumdar, Phys. Rev. Lett. **96**, 045901 (2006).

[10] N. A. Katcho, N. Mingo, and D. A. Broido, Phys. Rev. B **85**, 115208 (2012).

[11] A. Sparavigna, Phys. Rev. B **65**, 064305 (2002).

[12] A. Sparavigna, Phys. Rev. B **66**, 174301 (2002).

[13] D. A. Broido, M. Malorny, G. Birner, N. Mingo, and D. A. Stewart, Appl. Phys. Lett. **91**, 231922 (2007).

[14] A. Ward, D. A. Broido, D. A. Stewart, and G. Deinzer, Phys. Rev. B **80**, 125203 (2009).

[15] W. Li, J. Carrete, N. A. Katcho, and N. Mingo, Comput. Phys. Commun. **185**, 1747 (2014).

[16] Wu Li, N. Mingo, L. Lindsay, D. A. Broido, D. A. Stewart, and N. A. Katcho, Phys. Rev. B **85**, 195436 (2012).

[17] Wu Li, L. Lindsay, D. A. Broido, D. A. Stewart, and N. Mingo, Phys. Rev. B **86**, 174307 (2012).

[18] P. G. Klemens, Proc. Phys. Soc. A **68**, 1113 (1955).

[19] V. Kim and A. Majumdar, J. Appl. Phys. **99**, 084306 (2006).

[20] N. Mingo, K. Esfarjani, D. A. Broido, and D. A. Stewart, Phys. Rev. B **81**, 045408 (2010).

[21] A. Kundu, N. Mingo, D. A. Broido, and D. A. Stewart, Phys. Rev. B **84**, 125426 (2011).

[22] P. Chen, N. A. Katcho, J. P. Feser, Wu Li, M. Glaser, O. G. Schmidt, D. G. Cahill, N. Mingo, and A. Rastelli, Phys. Rev. Lett. **111**, 115901 (2013).

[23] T. Murakami, T. Shiga, T. Hori, K. Esfarjani, and J. Shiomi, Europhys. Lett. **102**, 46002 (2013).

[24] V. Gallina and M. Omini, Phys. Stat. Sol. **7**, 29 (1964).

[25] C. A. Ratsifaritana and P. G. Klemens, Int. J. Thermophys. **8**, 737 (1987).

[26] G. Xie, Y. Shen, X. Wei, L. Yang, H. Xiao, J. Zhong, and G. Zhang, Sci. Rep. **4**, 5085 (2014).

[27] A. A. Maradudin, G. H. Weiss, and E. W. Montroll, *Theory of Lattice Dynamics in the Harmonic Approximation* (Academic, New York, 1963).

[28] P. Sheng, *Introduction to Wave Scattering, Localization and Mesoscopic Phenomena* (Springer, Berlin, 2006).

[29] P. N. Keating, Phys. Rev. **145**, 637 (1966).

[30] Ph. Lambin and J. P. Vigneron, Phys. Rev. B **29**, 3430 (1984).

[31] G. Kresse and J. Furthmüller, Phys. Rev. B **54**, 11169 (1996).

[32] M. E. Newton, Electron Paramag. Reson. **20**, 131 (2007).

[33] P. R. Briddon and R. Jones, Phys. B (Amsterdam, Neth.) **185**, 179 (1993).

[34] E. B. Lombardi, A. Mainwood, K. Osuch, and E. C. Reynhardt, J. Phys. Condens. Matter **15**, 3135 (2003).

[35] M. Lanoo and J. Bourgoin, *Point Defects in Semiconductors I: Theoretical Aspects* (Springer, New York, 1981).

[36] A. Zywietz, J. Furthmüler, and F. Bechstedt, Phys. Status Solidi B **210**, 13 (1998).

[37] A. Togo, F. Oba, and I. Tanaka, Phys. Rev. B **78**, 134106 (2008).

[38] L. A. Turk and P. G. Klemens, Phys. Rev. B **9**, 4422 (1974).

[39] E. A. Burgemeister, Phys. B (Amsterdam, Neth.) **93**, 165 (1978).

[40] R. Berman, P. R. W. Hudson, and M. Martínez, J. Phys. C **8**, L430 (1975).

[41] A. J. Schorr, in *Proceedings of International Industrial Diamond Conference, Chicago, IL, USA, 20-22 October, 1969* (Industrial Diamond Association of America, Moorestown, NJ, 1970), p. 185.

[42] G. A. Slack, J. Phys. Chem. Solids **34**, 321 (1973).

[43] E. A. Burgemeister and C. A. J. Ammerlaan, Phys. Rev. B **21**, 2499 (1980).